Evidence for Carbonate Surface Complexation during Forsterite Carbonation in Wet Supercritical Carbon Dioxide

John S. Loring*, Jeffrey Chen, Pascale Bénézeth[a], Odeta Qafoku, Eugene S. Ilton, Nancy M. Washton, Christopher J. Thompson, Paul F. Martin, B. Peter McGrail, Kevin M. Rosso, Andrew R. Felmy, and Herbert T. Schaef

Pacific Northwest National Laboratory, Richland, WA 99352 USA

[a]*Géosciences Environnement Toulouse (GET), CNRS, UMR 5563, 14 Avenue Edouard Belin, 31400 Toulouse, France*

* Corresponding author. Phone: (509) 371-6743; fax: (509) 371-6354. Email address: john.loring@pnnl.gov

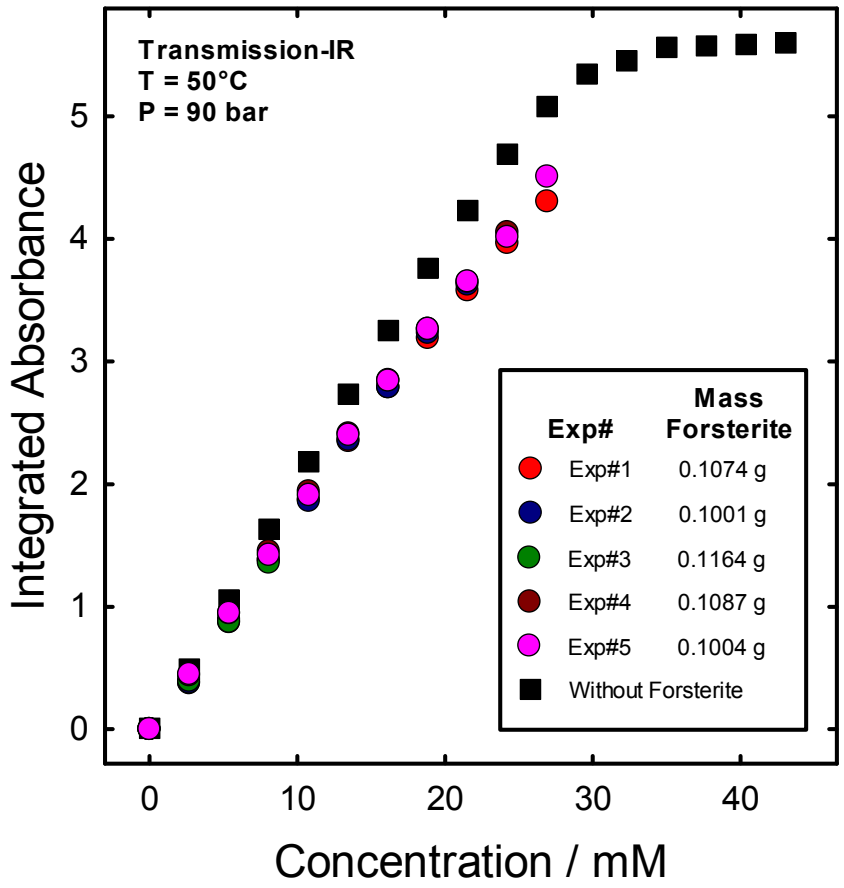

Figure S1. The integrated absorbance from *in situ* transmission IR under the HOH bending mode of H_2O dissolved in $scCO_2$ versus H_2O concentration for titrations of the empty high pressure IR cell (i.e. calibration curve, see text) and the cell containing forsterite (Exp#1-Exp#5, see Table I) at 50 °C and 90 bar.

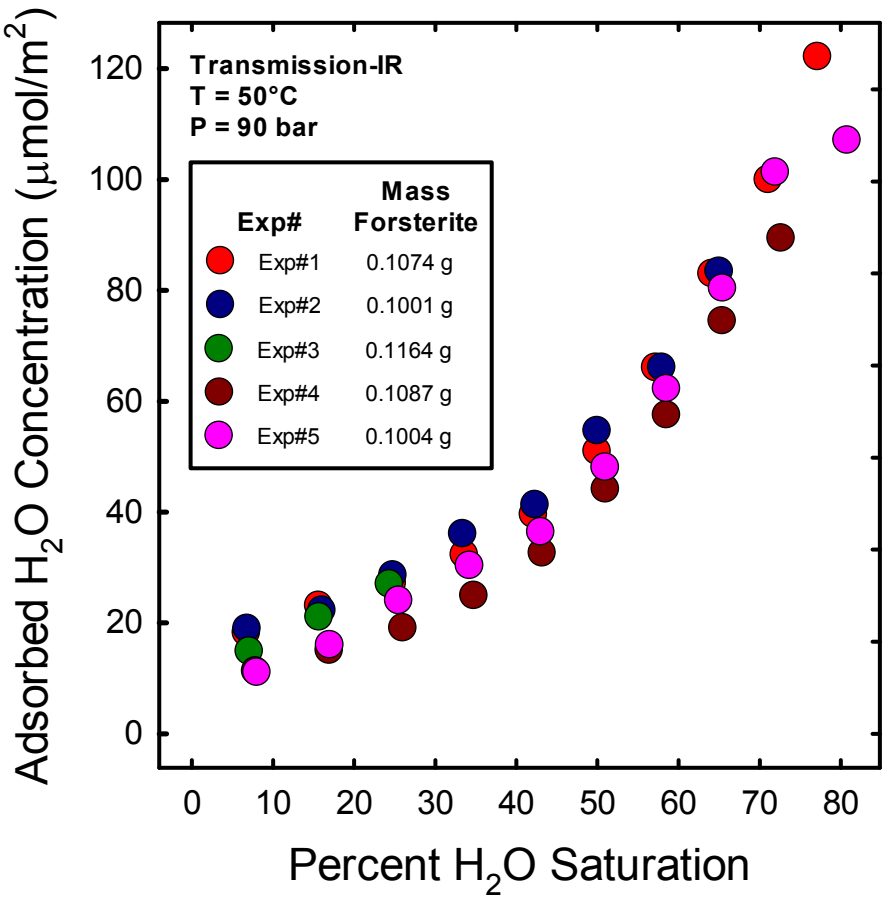

Figure S2. Adsorbed H_2O concentrations as a function of the percent H_2O saturation in the $scCO_2$ for titrations of forsterite (Exp#1-Exp#5, see Table I) with water at 50 °C and 90 bar. The precision in the sorbed H_2O concentrations is estimated ±10 µmol/m^2.

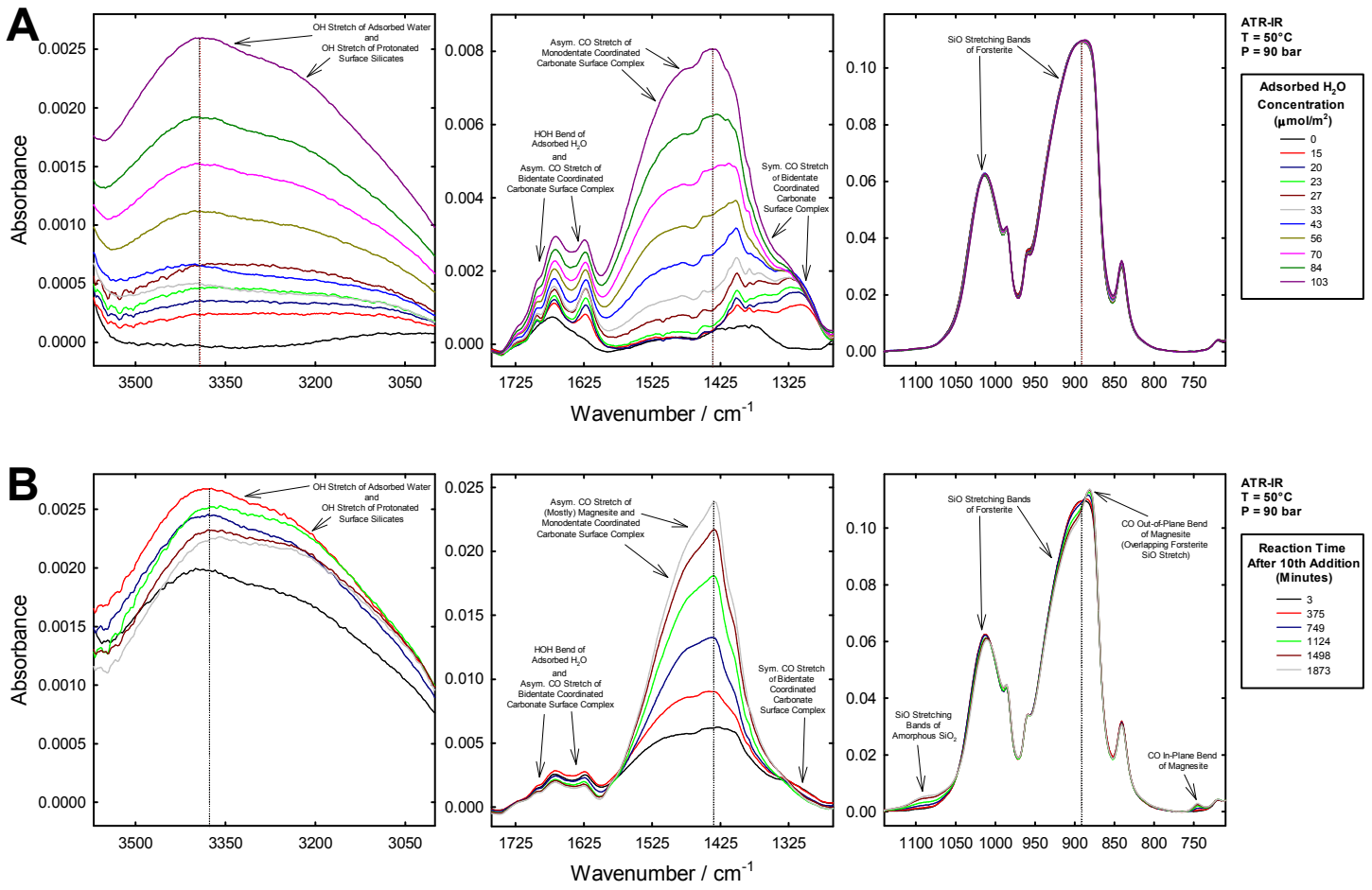

Figure S3. *In situ* ATR IR spectra as a function of (a) adsorbed H_2O concentration and (b) time after the 10th water addition (103 µmol/m^2 adsorbed H_2O) from Exp#1 where 0.1074 g of forsterite was titrated with water in $scCO_2$ at 50 °C and 90 bar (see Table 1). The background spectrum is the empty cell.

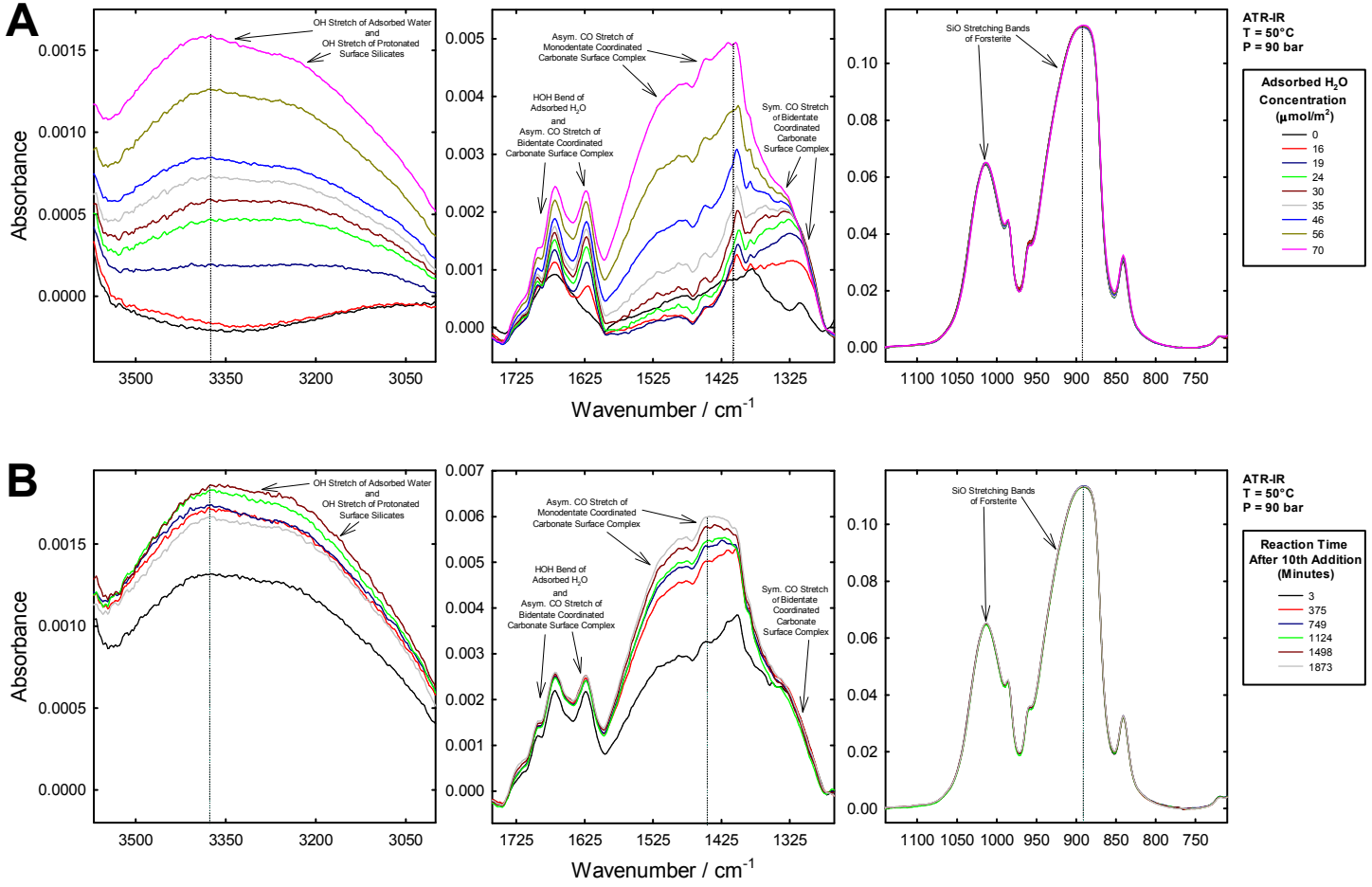

Figure S4. *In situ* ATR IR spectra as a function of (a) adsorbed H_2O concentration and (b) time after the 8th water addition (70 µmol/m^2 adsorbed H_2O) from Exp#2 where 0.1001 g of forsterite was titrated with water in $scCO_2$ at 50 °C and 90 bar (see Table 1). The background spectrum is the empty cell.

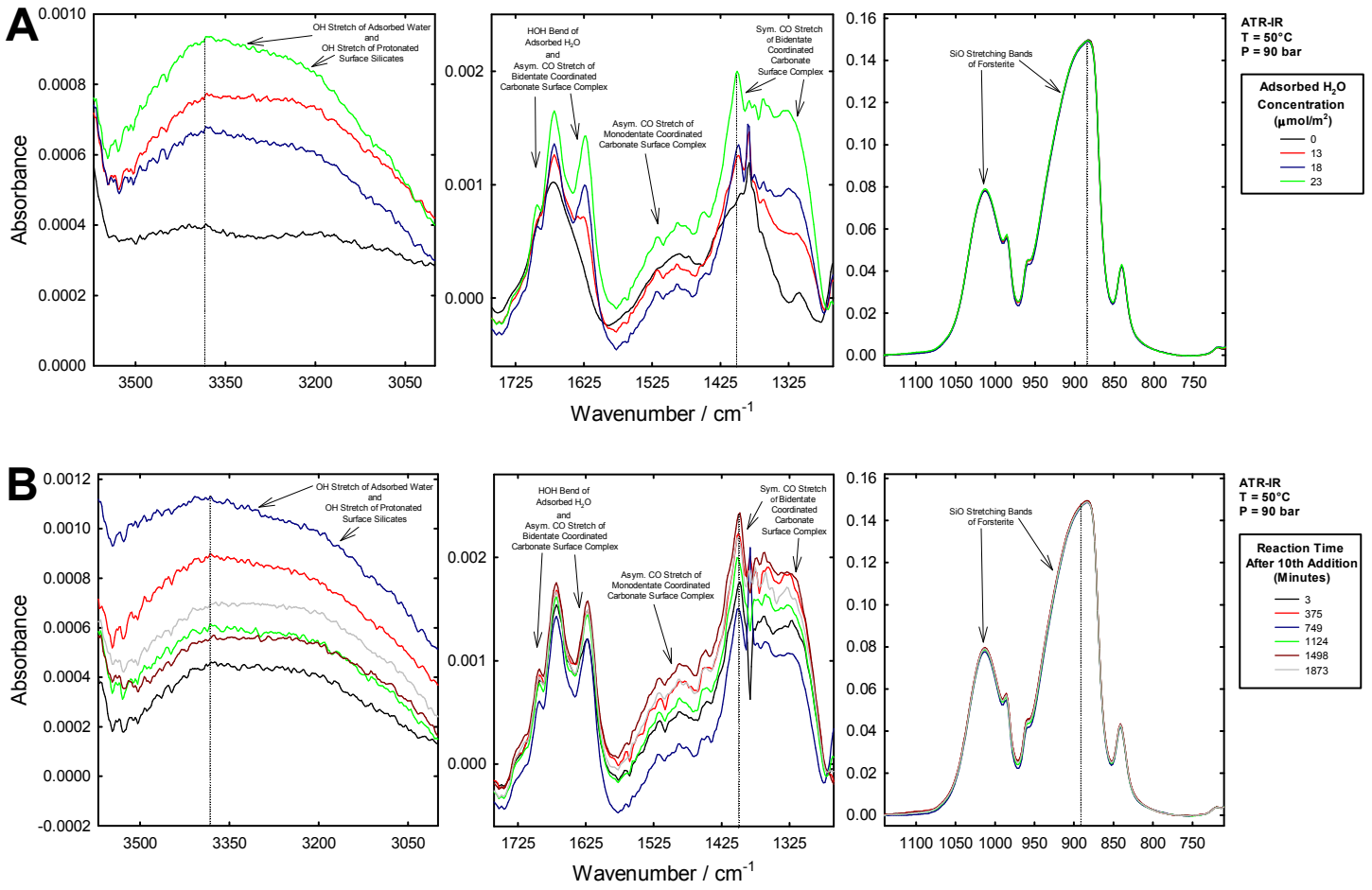

Figure S5. *In situ* ATR IR spectra as a function of (a) adsorbed H_2O concentration and (b) time after the 3rd water addition (23 µmol/m^2 adsorbed H_2O) from Exp#3 where 0.1064 g of forsterite was titrated with water in $scCO_2$ at 50 °C and 90 bar (see Table 1). The background spectrum is the empty cell.

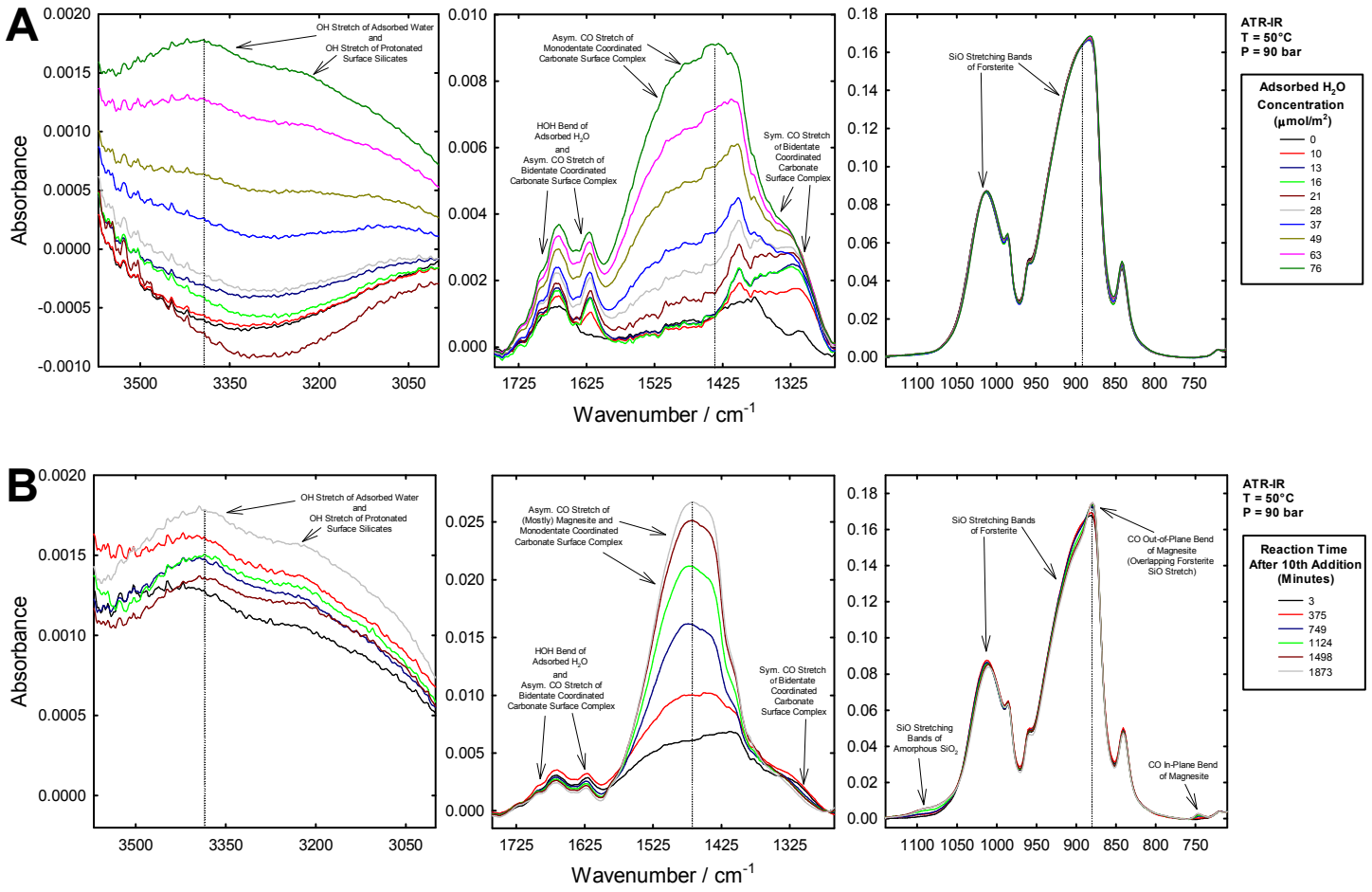

Figure S6. *In situ* ATR IR spectra as a function of (a) adsorbed H_2O concentration and (b) time after the 9th water addition (76 µmol/m^2 adsorbed H_2O) from Exp#4 where 0.1087 g of forsterite was titrated with water in $scCO_2$ at 50 °C and 90 bar (see Table 1). The background spectrum is the empty cell.

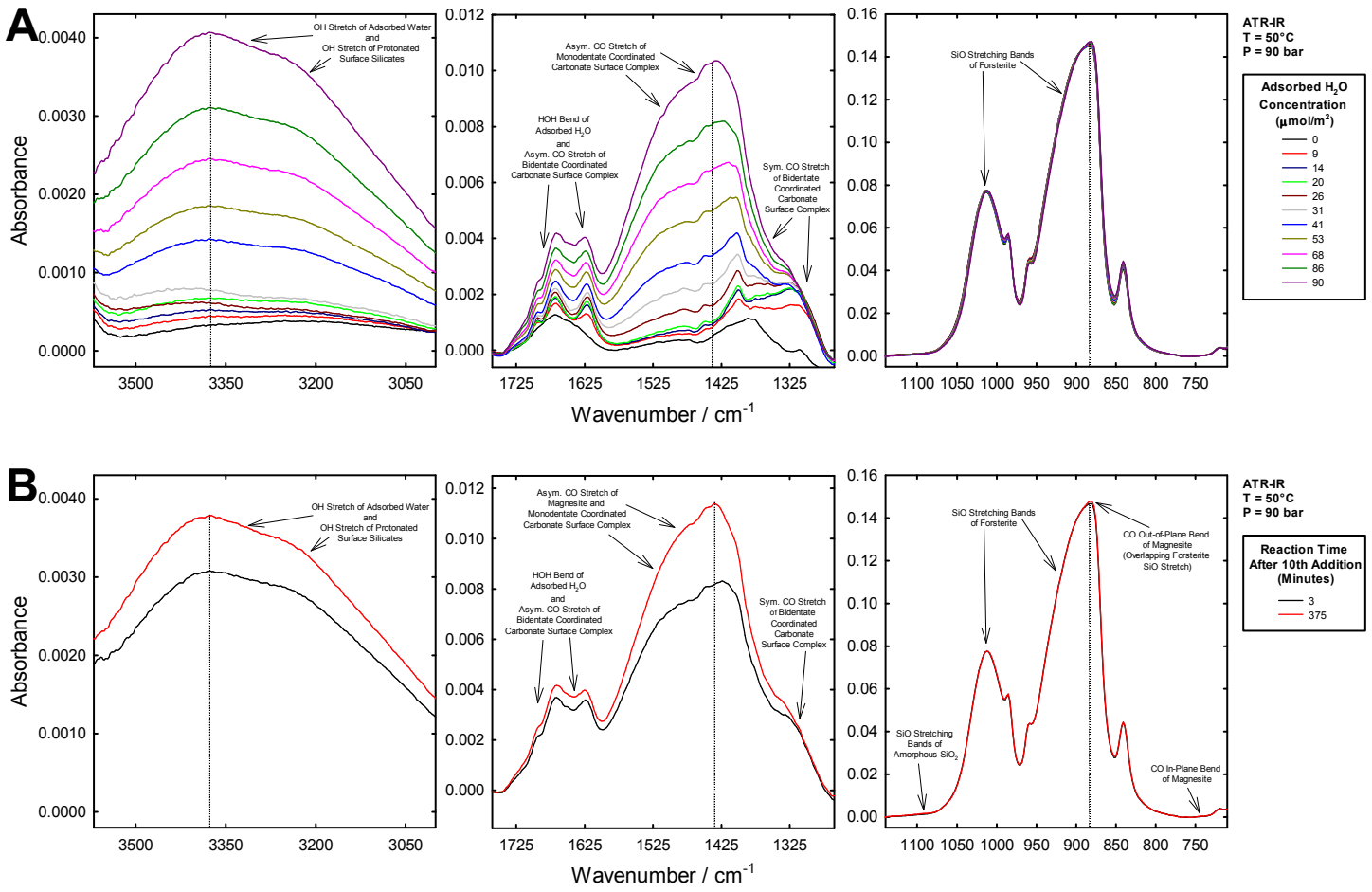

Figure S7. *In situ* ATR IR spectra as a function of (a) adsorbed H_2O concentration and (b) time after the 10th water addition (90 µmol/m^2 adsorbed H_2O) from Exp#5 where 0.1004 g of forsterite was titrated with water in $scCO_2$ at 50 °C and 90 bar (see Table 1). The background spectrum is the empty cell.

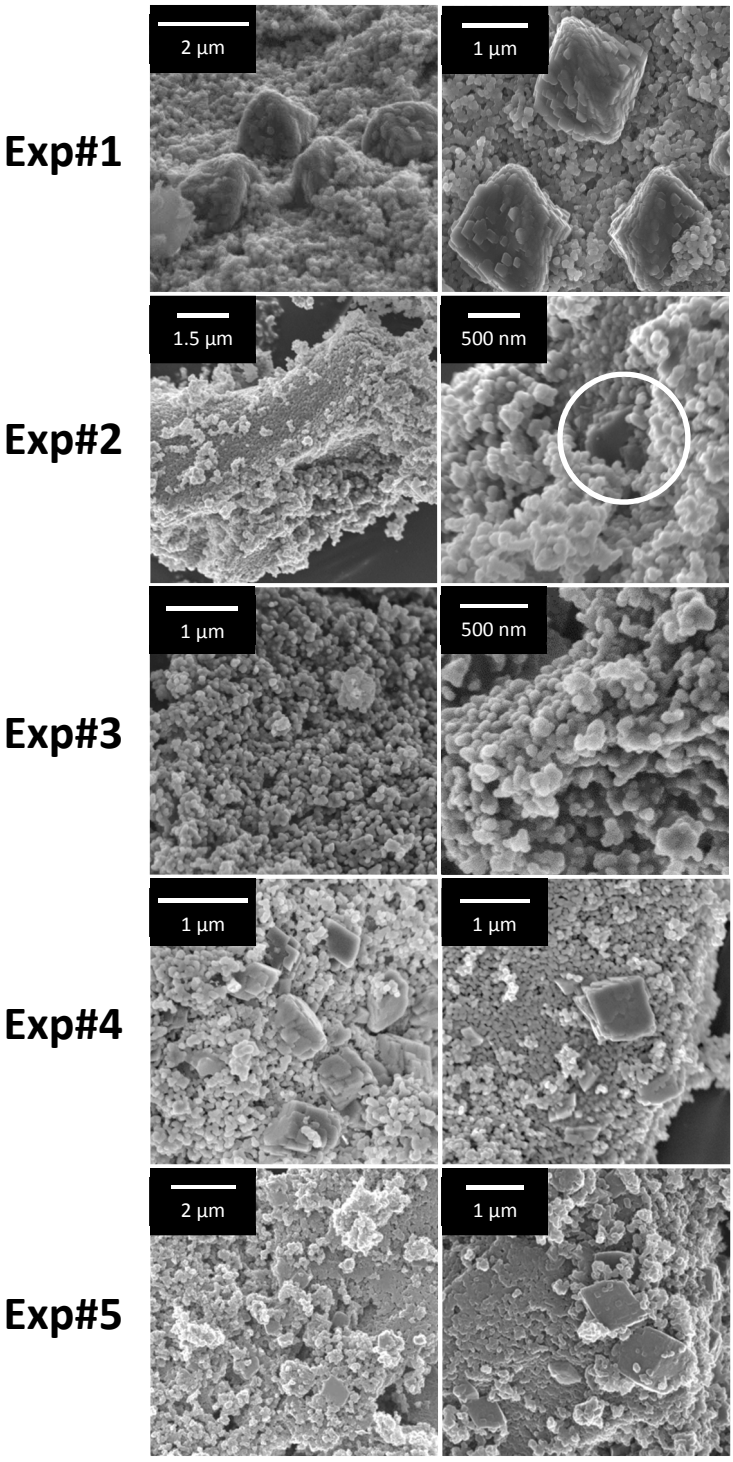

Figure S8. *Ex situ* SEM images of the post-reacted samples from Exp#1-Exp#5 where forsterite was titrated with water in $scCO_2$ at 50 °C and 90 bar (see Table 1). These images are of the samples scraped from their microscope slide substrate.

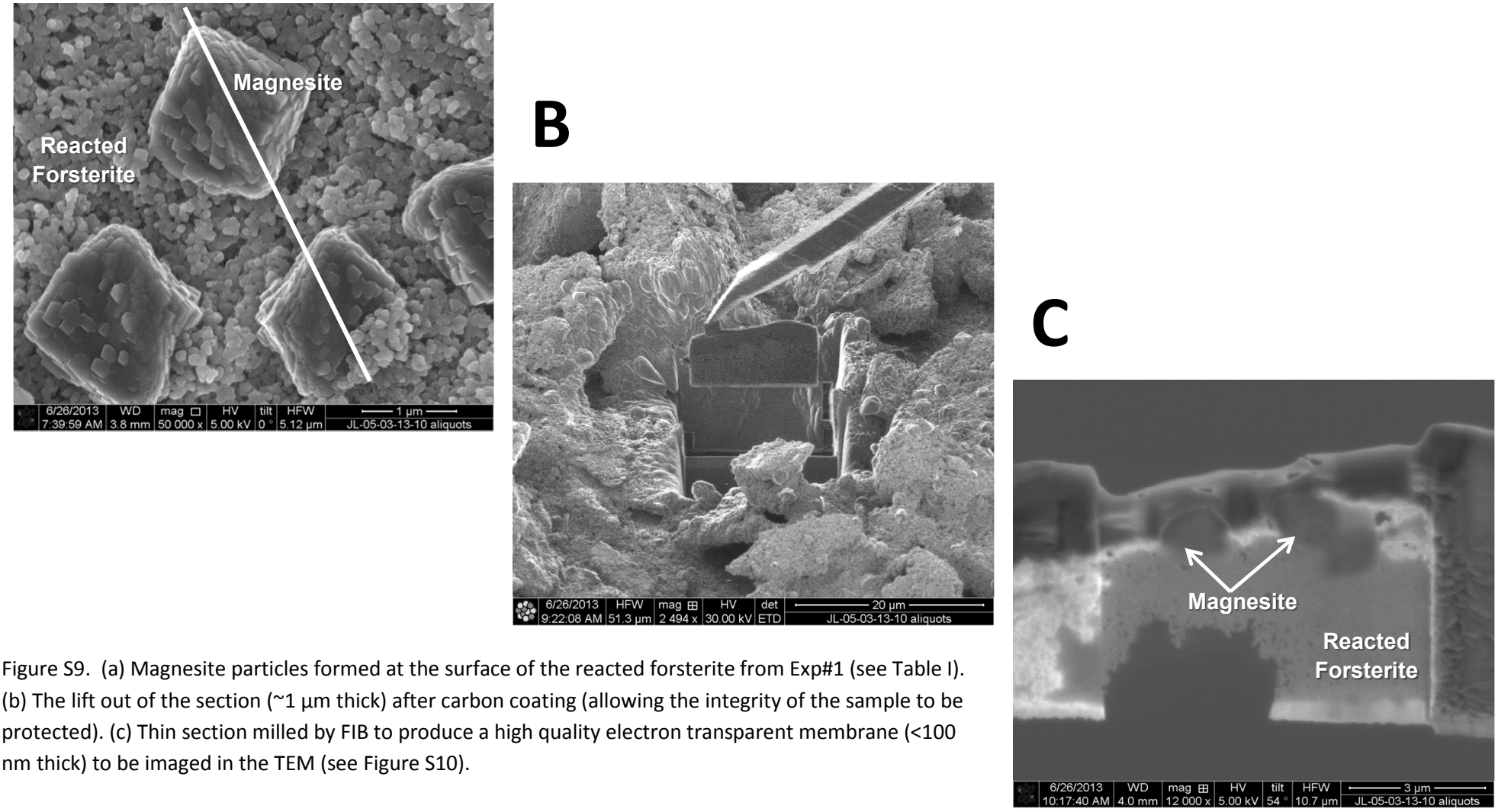

Figure S9. (a) Magnesite particles formed at the surface of the reacted forsterite from Exp#1 (see Table I). (b) The lift out of the section (~1 µm thick) after carbon coating (allowing the integrity of the sample to be protected). (c) Thin section milled by FIB to produce a high quality electron transparent membrane (<100 nm thick) to be imaged in the TEM (see Figure S10).

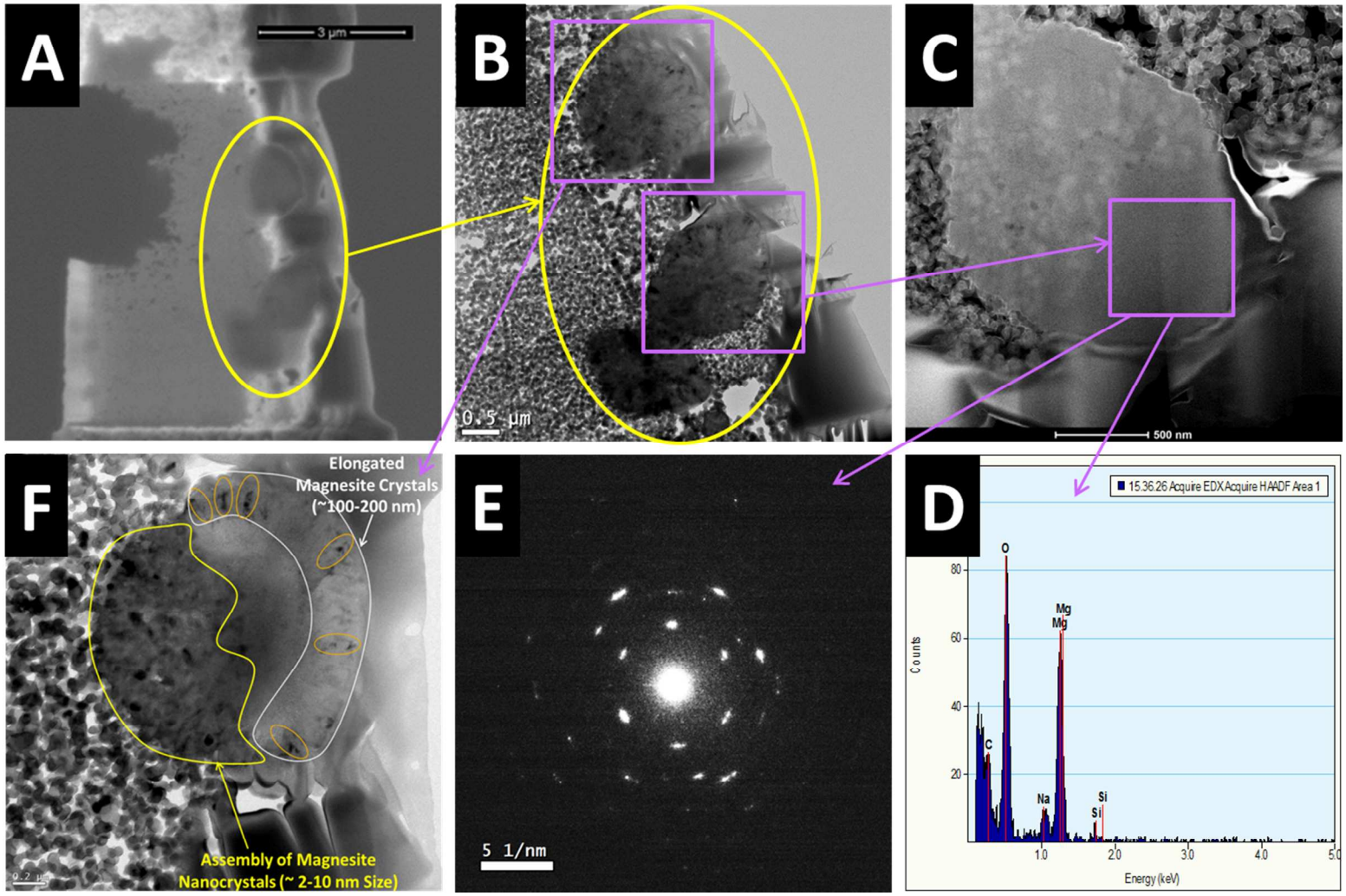

Figure S10. Results of TEM analyses performed on the thin section obtained from SEM-FIB as described in Figure S9. (a) Same thin section as shown in Figure S9c. (b) (c) and (f) TEM bright field images of the thin section demonstrating that the magnesite particles (seen by SEM, Figure S9a) are in fact an assembly of nanocrystals with different size (f): i) ~2-10 nm size embedded in the nanoforsterite, filling its pore space; ii) elongated magnesite crystals toward the bulk surface of ~ 100-200 nm size, which growth in different orientation in accordance with the SAED (selected-area electron diffraction) pattern shown in (e) and iii) in between the two crystals dimensions probably intermediate sizes of magnesite. Both the acquired EDX (d) and the d spacing obtained from the SAED (d1(-120)=2.376 Å, d2(110)=2.38 Å et d3(030)=1.36 Å) (e) demonstrating that the carbonate formed is crystalline magnesite.

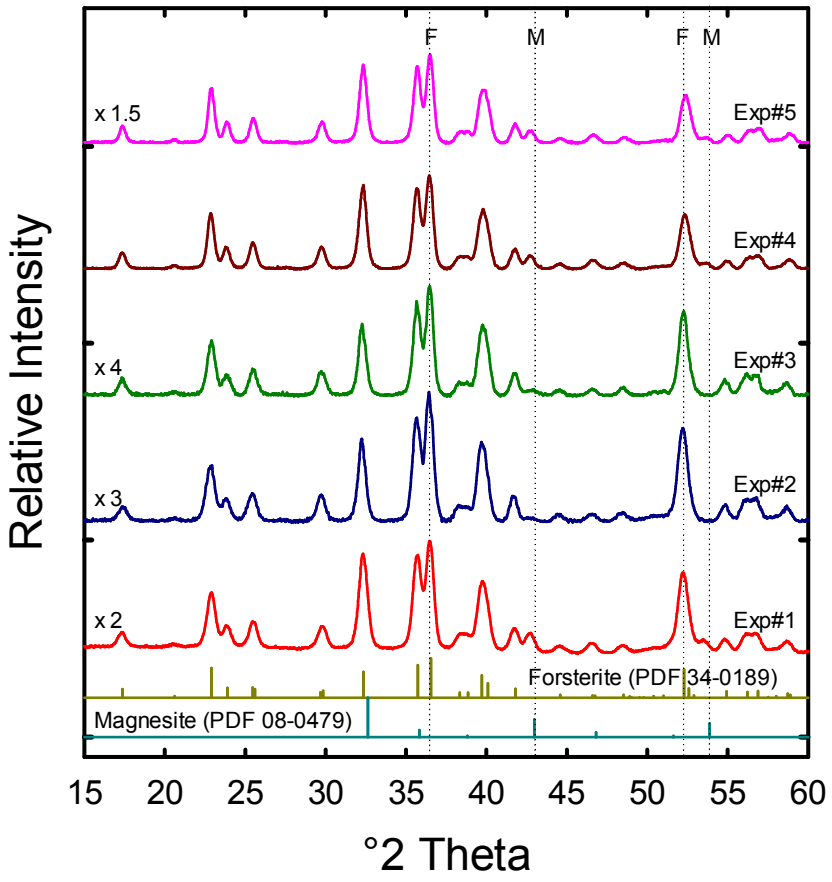

Figure S11. *Ex situ* X-ray diffraction tracings of post-reacted samples from Exp#1-Exp#5 where forsterite was titrated with water in $scCO_2$ at 50 °C and 90 bar (see Table 1).

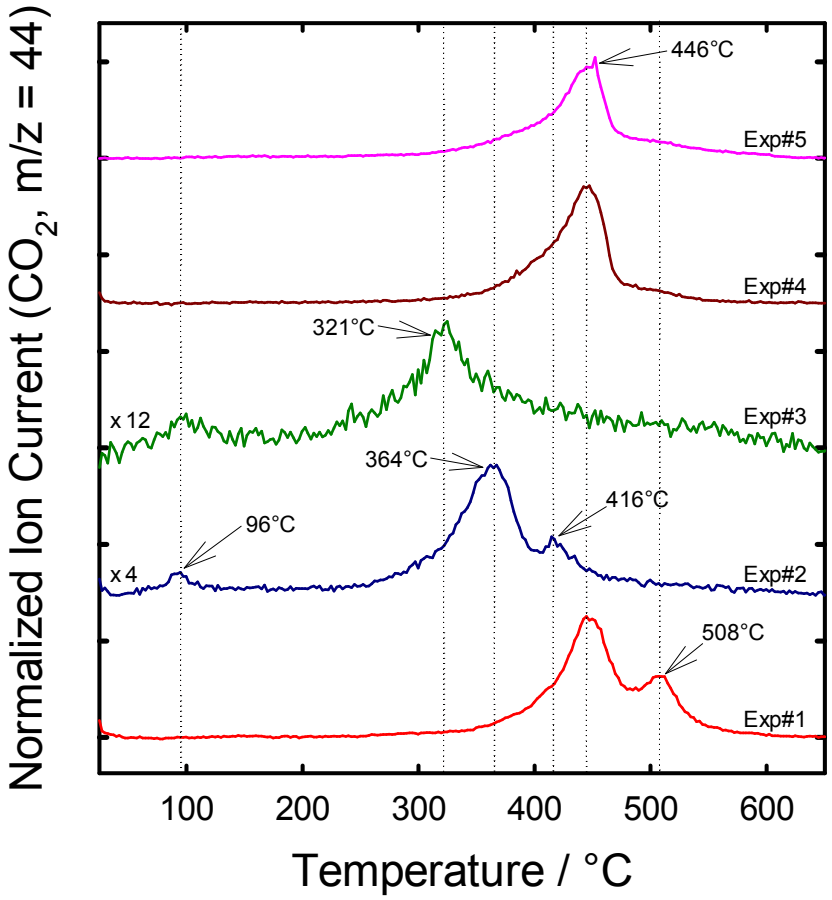

Figure S12. *Ex situ* TGA-MS of post-reacted samples from Exp#1-Exp#5 where forsterite was titrated with water in $scCO_2$ at 50 °C and 90 bar (see Table 1).

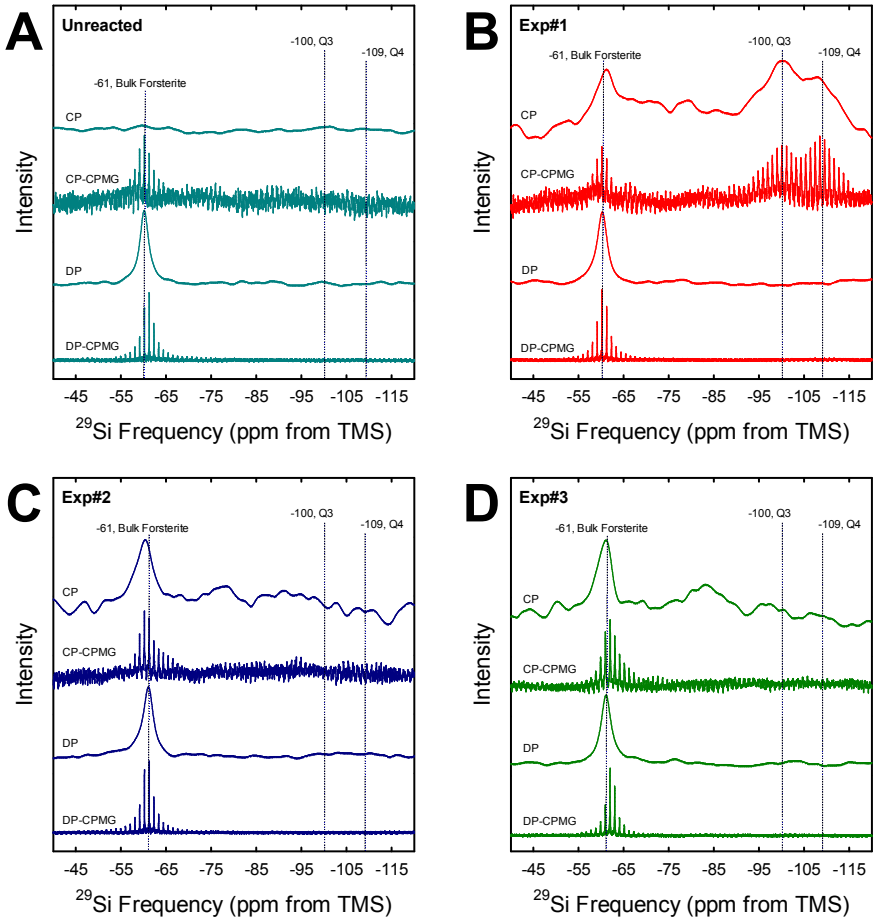

Figure S13. *Ex situ* ^{29}Si direct polarization (DP) with ^{1}H decoupling and ^{1}H-^{29}Si cross polarization (CP) MAS-NMR of (a) unreacted forsterite and post-reacted samples from (b) Exp#1, (c) Exp#2, and (d) Exp#3 where forsterite was titrated with water in $scCO_2$ at 50 °C and 90 bar (see Table 1). The Carr Purcell Meiboom Gill (CPMG) sequence was coupled to both DP and CP experiments (DP-CPMG and CP-CPMG) to enhance sensitivity.

Table SI. X-Ray Photoelectron Spectroscopy (XPS) Results[a].

	Si2p			O1s								
	Forsterite	**SiO_2**	**SiO_xH_n**	**Forsterite**	**CO_3**	**SiO_2**	**H_2O[b]**	**H_2O[c]**	**Mg/Si(tot)**	**Mg/Si(forsterite)**	**CO_3/Mg**	**CO_3/Si(tot)**
Unreacted Forsterite												
Binding Energy (eV)	101.5	103.1	nd	530.6	531.8	532.6	nd	nd				
%	90.89	9.1		80.44	10.8[e]	8.7			1.79	1.97	0.081	0.146
Exp#1[d]												
Binding Energy (eV)	101.9	103.5	104.1	531.2	531.7	532.4	533.5	534.5				
%	62.3	32.2	5.54	32.9	8.6[e]	29.3	18.3	8.2	1.17	1.77	0.075	0.088
Exp#2												
Binding Energy (eV)	101.8	103.2	nd	530.9	532.0	532.9	nd	nd				
%	89.2	10.8		74.7	15.7[e]	8.32			1.66	1.86	0.120	0.198
Exp#3												
Binding Energy (eV)	101.7	103.0	nd	530.9	532.0	532.8	nd	nd				
%	89.8	10.2		74.0	15.4[e]	8.3			1.77	1.97	0.115	0.203

[a] tot = total, nd = not detected, % = atomic percent, [b] chemisorbed H_2O, [c] physisorbed H_2O, adventitious C-O not shown. [d] Note that the O1s line was considerably broadened relative to the other samples and that despite including more components in the fit, each component still had a larger FHWM than for the other samples; this implies that there are unresolved components and that the designation of each component is less certain. [e] Concentration is fixed using the fitted C1s line for carbonate.

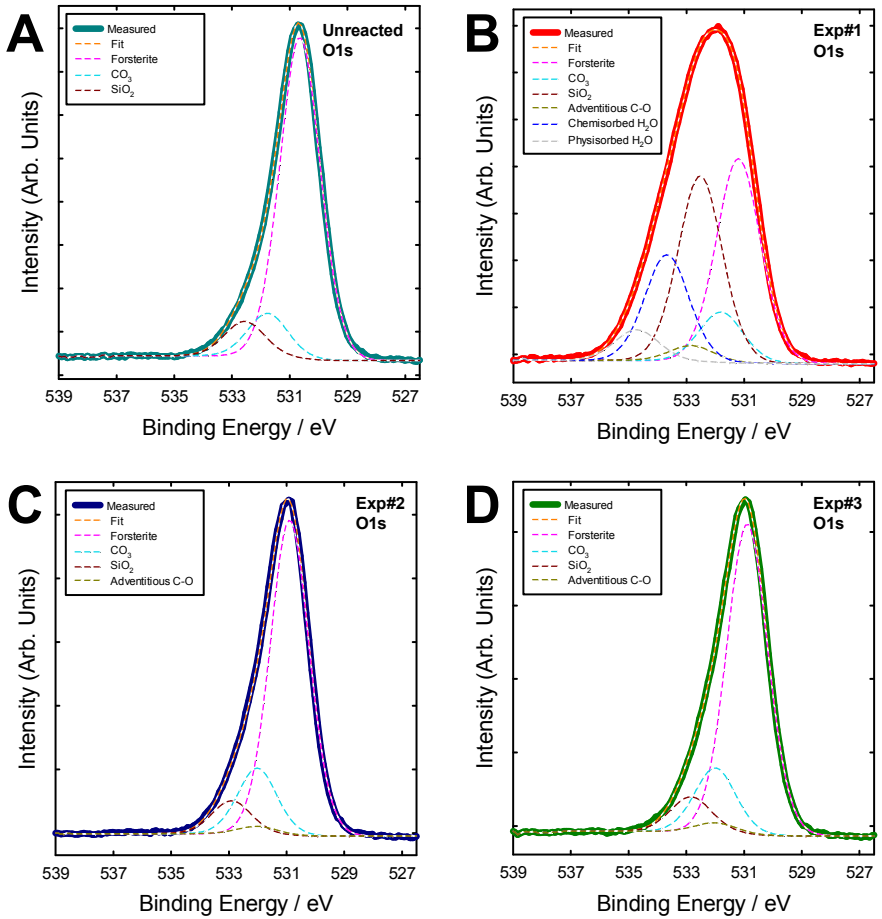

Figure S14. *Ex situ* O1s XPS of (a) unreacted forsterite and post-reacted samples from (b) Exp#1, (c) Exp#2, and (d) Exp#3 where forsterite was titrated with water in $scCO_2$ at 50 °C and 90 bar (see Table 1).

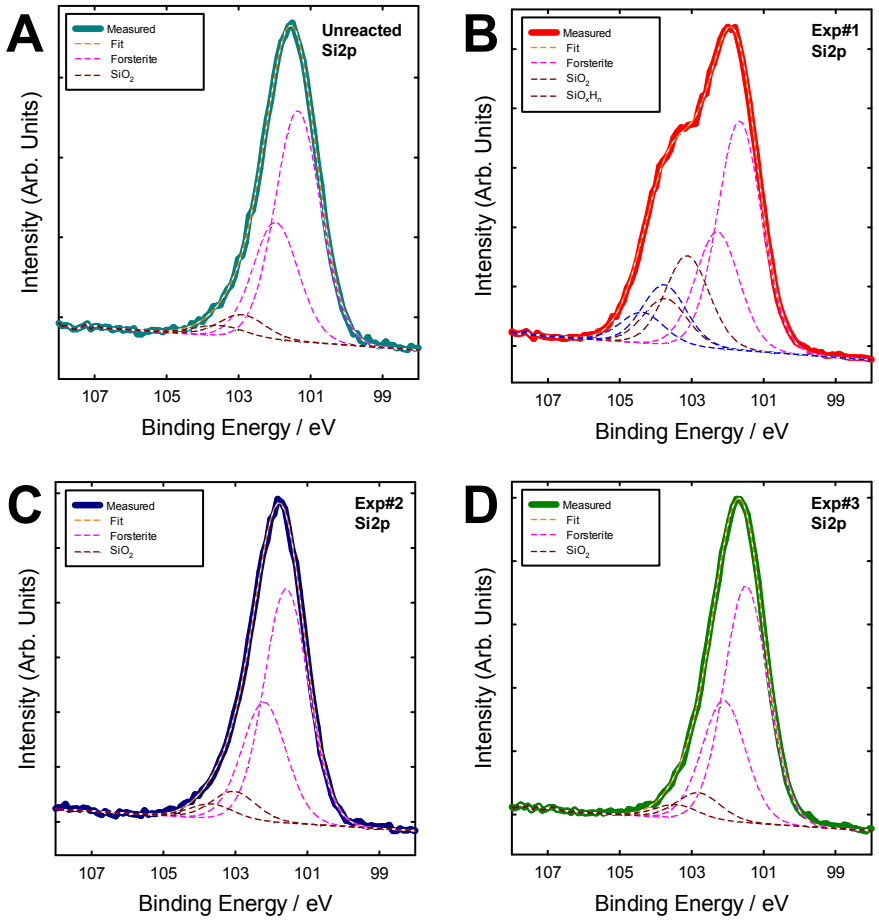

Figure S15. *Ex situ* Si2p XPS of of (a) unreacted forsterite and post-reacted samples from (b) Exp#1, (c) Exp#2, and (d) Exp#3 where forsterite was titrated with water in $scCO_2$ at 50 °C and 90 bar (see Table 1).